Journal of Water Process Engineering 9 (2016) 208–214

Contents lists available at ScienceDirect

Journal of Water Process Engineering

journal homepage: www.elsevier.com/locate/jwpe

Removal of fine iron-oxide particles after post-filtration in local potable water using an electrophoretic method

M.Nazli Naim[a,*], Yeon Hui Ting[a], Rabitah Zakaria[a], Azhari Samsu Baharuddin[a], Khairul Faezah Md. Yunos[a], Noor Fitrah Abu Bakar[b,c], I.Wuled Lenggoro[d]

[a] Faculty of Engineering, Department of Process and Food Engineering,Universiti Putra Malaysia, Selangor 43400, Serdang, Malaysia
[b] Faculty of Chemical Engineering, Universiti Teknologi MARA, 40450, Shah Alam, Malaysia
[c] CoRe of Frontier Material and Industrial Applications, Universiti Teknologi MARA, 40450, Shah Alam, Malaysia
[d] Graduate School of Bio-Applications and Systems Engineering and Department Chemical of Engineering, 2-24-16 Nakacho, Koganei, Tokyo 184-8588, Japan

ARTICLE INFO

Article history:
Received 3 August 2015
Received in revised form 4 January 2016
Accepted 10 January 2016

Keywords:
Electrophoretic deposition
Fibre electrodes
Limiting flux
Iron oxide
Zeta potential

ABSTRACT

Potable water from several residential areas on the east coast of Malaysia was filtered using a polyethersulphone (PES) membrane to separate the coarse and fine iron-oxide particles inside the pipelines. The as-received samples consisted of a wide distribution of particle sizes, ranging from 5 μm to 400 nm. The concentration of fine iron-oxide particles inside a distribution system was extremely low. Hence, a specific method is necessary to concentrate and separate the fine particles from the coarse ones. To study the fine particles from the bulk, excess pressure was applied to the membrane filter so that the clogged particles were released into the permeate. A 100 kDa PES membrane was used to separate the particles, because the samples consisted of a wide molecular-weight cut-off range from 89 g/mol goethite (α-FeOOH) to 231 g/mol hematite (Fe_2O_3). After the filtration process, the size distribution of permeated particles reduced to 550–400 nm. Through X-ray diffraction analysis, numerous polymorphs such as α-FeOOH, Fe_3O_4, Fe_2O_3 and maghemite were detected from the samples. The zeta potential value of the permeated particles changed from −18.5 to −13 mV, suggesting that the dispersity of permeated iron-oxide particles became unstable, but remained adequate for electrophoretic deposition (EPD). The fibrous carbon electrode used in the EPD process, could remove up to 87% of the permeated iron-oxide particles compared to solid carbon electrodes (<56%). A high-surface-area, porous electrode and a moderate applied voltage were preferred in order to minimise gas formation, reduce the electro-osmosis effect and increase the deposition efficiency.

1. Introduction

Drinking water, or potable water, is defined as treated water that is used for domestic purposes such as drinking, cooking and personal hygiene. It is safe for consumption by humans with low risk of immediate or long-term harm. In tropical regions such as Malaysia, potable water is distributed using pipelines that are made from iron-based materials. During the distribution process, deterioration of the inner pipe interface occurs, owing to corrosion, contributing to the accumulation of iron-oxide particles in the bulk. At the initial stage of the corrosion process, the solid iron oxides exist in low-crystalline form, but over time, the compounds transform into higher crystalline forms, such as goethite (α-FeOOH) or hematite (Fe_2O_3). Dixit and Hering pointed out that the rate of these transformations depends on temperature, pH and the presence of other co-occurring solutes [1]. During the corrosion process, the morphology of the inner iron pipe surfaces consists of a porous core, a hard shell layer (HSL) and a surface layer. The porous core regions consist of enormous fine tubercles that are composed of α-FeOOH, lepidcrocite (γ-FeOOH), green rusts, magnetite (Fe_3O_4), Fe_2O_3, ferrous hydroxide [$Fe(OH)_2$], ferric hydroxide [$Fe(OH)_3$] and siderite ($FeCO_3$). The HSL lies on top of the core region and varies from one to a few millimeters in thickness [2], and it is typically composed of Fe_3O_4 and α-FeOOH [3,4]. Generally, the outermost or surface layer can be up to several millimeters thick. The layer is more heterogeneous and can contain α-FeOOH, γ-FeOOH, $Fe(OH)_3$, silicates, phosphates and carbonates [5]. Sarin et al. and Senftle et al. explained that, under ambient conditions, the corrosion process is

* Corresponding author.
E-mail address: mohdnazli@upm.edu.my (M.Nazli Naim).

http://dx.doi.org/10.1016/j.jwpe.2016.01.006
2214-7144/

dominated by iron ionisation followed by solid reduction before the iron is released as a solid ferrous form [4,6]. Later, it could either be dispersed in the bulk or deposited as a scale on the pipe-wall surface [7,16]. The solid fragment of iron-oxide substances or tubercles that are released into the potable water initially exist in the milimeter-to-submicron size order. The coarse tubercles are easy to sediment, but the fine tubercles are well-dispersed and can flow homogeneously inside pipelines or distribution systems. Fine iron-oxide particles that exist in the nanometer size order have a higher surface activity compared to coarse ones, and have the potential to form natural adsorbent particles. As a result, the fine tubercles that are exposed with a long residence time inside a distribution system will turn into coarse particles with the potential of promoting biofilm growth, microbial algae activities [3,8], green rust [9] and adsorption or accumulation of some contaminant such as arsenic [10] and radium [11].

The concentration of fine iron-oxide particles inside a distribution system is extremely low and difficult to study. In order to study the particles, a specific method is necessary to concentrate and separate the fine particles from the coarse ones. In the present study, a batch filtration process is used to increase the concentration of iron-oxide particles. The collected iron-oxide particles were filtered and trapped inside a membrane matrix. By increasing the applied pressure to slightly more than the limiting flux value, the fine iron-oxide particles that were trapped in the matrix were released to the permeate and could be measured and studied. The released iron-oxide particles were subjected to a removal process by means of electrophoretic deposition. According to Naim et al., electric-assisted separation or electrophoretic deposition (EPD) was conducted, because of its potential to be applied directly, without any additional treatment or chemicals [12]. However, before EPD could be applied, a preliminary study on the characterisation of permeated iron-oxide particles that were released to the permeate was necessary. This study also emphasised the potential of removing and depositing the permeated iron-oxide particles after applying the EPD system in terms of removal efficiency and deposit-substrate morphology. Characterisation of fine iron-oxide particles in the pre- and post-filtration steps is important in order to study the feasibility of applying EPD in the permeate region or after the filtration process. In this study, a particular concern was given to the permeation of iron-oxide particles and the surface charge of the iron-oxide particles after passing the membrane. The EPD process is preferable if the permeated iron-oxide particles have a high surface charge or adequate zeta potential value. If the surface charge is completely stripped off by the membrane matrix, an additional treatment might necessary to increase the surface charge of the particles. Particular concerns when studying the separation parameters, such as limiting flux and applied pressure, are taken into account so that losses of particle charges through concentration polarisation and friction within the membrane matrix can be minimised. At the end of this work, an alternative method to increase the concentration of fine iron oxides removed by EPD was also demonstrated by increasing the electrode surface area and porosity.

2. Experimental

2.1. Collection of samples

A volume of 10 L of potable water was taken from several residences in Kuantan, Pahang, Malaysia. The tap water was collected in plastic bottles and tightly closed to prevent interaction with the surrounding environment. The taps and the pipelines were estimated to be about 10 years old and have a diameter of 2.5 cm. Both the taps and the pipes were made from galvanised iron (BS1387:1967). The collected water samples were tested according to the national standards for water quality (Malaysian standard), as shown in Table 1 [28].

Table 1
Analysis of the as-received samples according to the Malaysian Food Act, Water and Packaged Drinking Water Standard (Health) [28].

Parameter	Results, g/m^3	Standard, g/m^3
Colour	<2.5	15
Turbidity	1.5	5
pH	6.5	6.5–8.5
Aluminium, mg/L	Not detected (<0.06)	0.2
Arsenic, mg/L	Not detected (<0.0001)	0.05
Cadmium, mg/L	Not detected (<0.003)	0.005
Chromium, mg/L	Not detected (<0.03)	0.05
Copper, mg/L	0.05	1.0
Cyanide, mg/L	Not detected (<0.003)	0.1
Fluoride, mg/L	Not detected (<0.01)	1.5
Total hardness, mg/L	1.36	500
Iron, mg/L	0.05	0.3
Lead, mg/L	0.01	0.05
Magnesium, mg/L	0.16	150
Manganese, mg/L	Not detected (<0.002)	0.001
Mercury, mg/L	Not detected (<0.0001)	0.001
Mineral oil, mg/L	Not detected (<0.1)	0.3
Nitrate, mg/L	0.16	10
Phenol, mg/L	Not detected (<0.001)	0.002
Residual Chlorine, mg/L	Not detected (<0.1)	0.1
Selenium, mg/L	Not detected (<0.0001)	0.01
Silver, mg/L	Not detected (<0. 005)	0.05
Sodium, mg/L	0.82	200
Sulfur, mg/L	Not detected (<0. 01)	400
Zinc, mg/L	0.05	5

2.2. Filtration unit and membrane selection

A membrane made of polyethersulphone (PES) with an active surface area of 40 cm^2 was used as a filter for the filtration process. The filtration unit and the membrane system were purchased from Sartorius Stedim Malaysia Sdn. Bhd, Malaysia. The membrane had a 10 nm pore size with a 100 kDa molecular weight cut-off (WMCO). The process flow of membrane filtration from the source until the analysis stage is shown in Fig. 1.

2.3. Concentration of iron-oxide particles

The concentration of iron-oxide particles for samples as-received, permeated and remaining after the deposition was measured using ICP-OES (iCAP6000, Thermo Scientific, USA). The removal percentage calculation was performed to identify the EPD efficiency. The inductively coupled plasma was used to identify the metal element. The nitric acid digestion method was performed to reduce the particulates in order to form free ions.

2.4. X-ray diffraction (XRD) analysis

Each batch of the water samples was pre-filtered using a 0.2 μm polytetrafluoroethylene (PTFE) syringe filter. The purpose of pre-filtration is to avoid uncontrolled clogging, owing to the very wide particle size distribution. The process also removes unwanted contaminants such as debris and coarse natural organic matter (NOM), so that membrane filter clog can be minimised [13]. The thin film of membrane with accumulated particles was calcined in the furnace at 600 °C for 5 hours, and then preserved in the furnace for several hours in order to promote the crystallisation process [14]. The calcinated powders were analysed using an X-ray diffractometer (Model APD 2000, G.N.R., Italy). A copper anode was used as a radiation source (CuKα) with a wavelength of 1.54 nm. A voltage of 40 kV and current of 30 mA were used in XRD analysis [13]. The XRD analysis was perfor ed with scanning angles between 2 and 80°

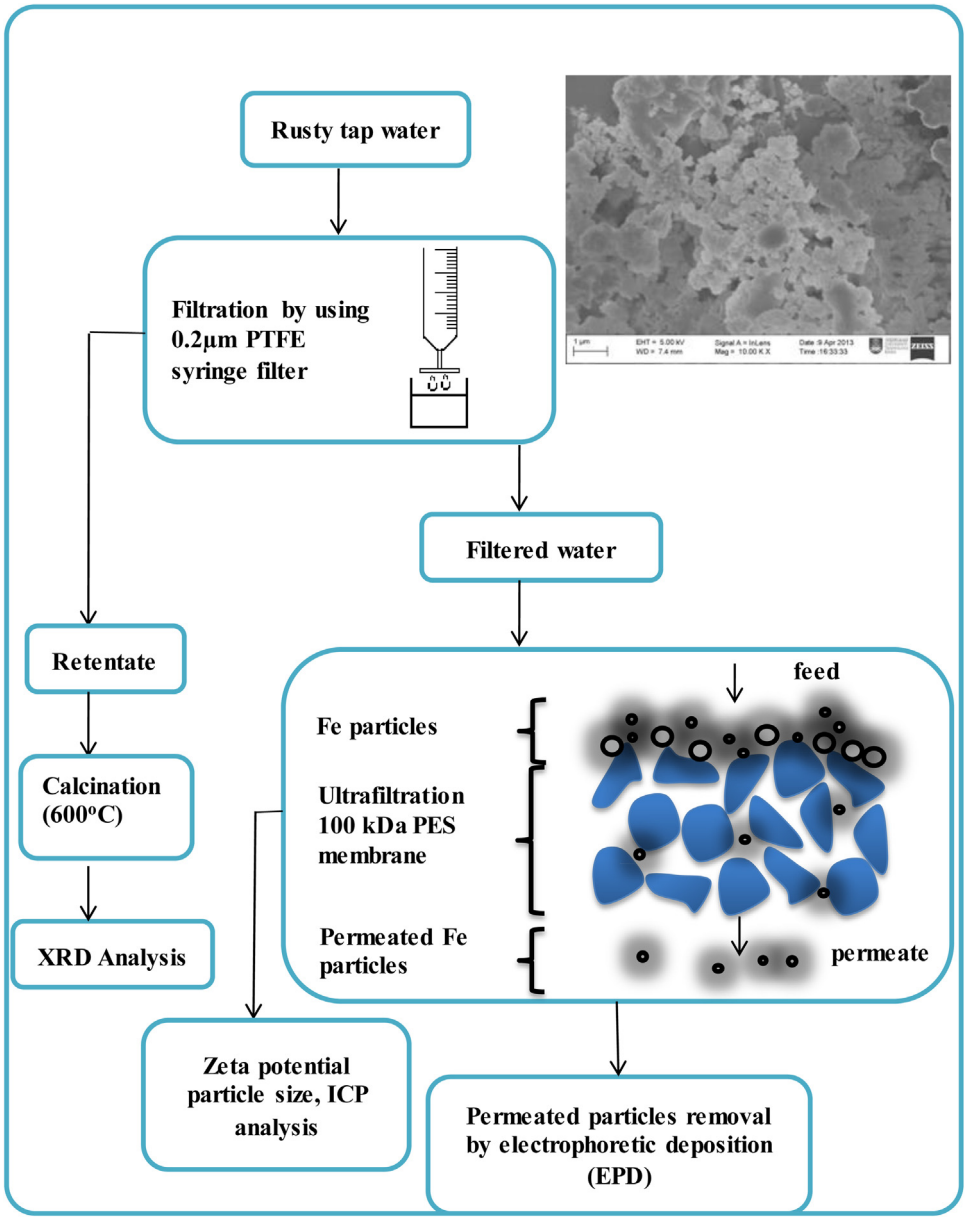

Fig. 1. Schematic illustration of the experimental method and the conducted analyses. Small SEM image at the top right indicates the collected iron-oxide tubercles. Electrophoretic deposition (EPD) was conducted after the filtration process.

and the speed was set at 2°/sec with step scans at 0.05° [14]. The generated peaks were analysed to identify the types of substance and other polymorphs available in the samples.

2.5. Membrane filtration

The membrane unit purchased from Sartorius (Vivacell 250, Germany) consists of sample reservoir, permeate container, PES membrane (100 kDa MWCO), pressure indicator and an inlet valve for compressed-air supply. The membrane was inserted into the sample reservoir with the volume marking facing the transparent slot. The water samples were kept inside the sample reservoir and capped with the pressure head. To observe the applied pressure, a gauge was installed on the valve that was connected to compressed air. An oil-free air compressor was installed in order to avoid oil or debris contamination during the filtration process. The inlet pressure was applied from 0.5 to 3.5 bar. A beaker was placed under the membrane unit to collect any discharged permeate.

2.6. Deposition and removal of iron-oxide particles

Carbon plates ($25 \times 5\,mm^2$) were submerged into 50 mL of the collected permeate water samples. The substrate distance and deposition time were set at 30 mm and 10 min, respectively. An electric field was applied using a direct current (DC) during the EPD. During the EPD, three different values of supply voltage; 5, 15 and 25 V, were applied to the samples. The distance between both electrodes was fixed at 2 cm. Details about the experimental setup are available from our previous work [12,30]. The same EPD process was also applied, using fibrous carbon substrates as a comparison to the earlier method. The deposits that attached to the substrates were dried for 5 h in a vacumm oven at 60 °C. To determine the iron-oxide removal, Eq. (1) was applied after the EPD process [12,30].

$$\text{Removal}(\%) = \frac{C_i - C_f}{C_i} \times 100 \quad (1)$$

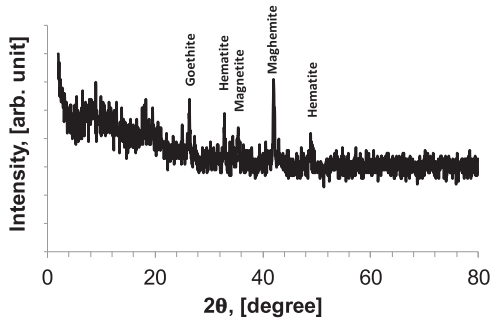

Fig. 2. XRD analysis of dried solid content collected on the pre-filtered surface (calcined at 600 °C, 5 h).

Where C_i (g/m^3) is the initial concentration and C_f (g/m^3) is the final concentration of iron (Fe) after the EPD process.

2.7. Zeta-potential measurements

Each sample was measured with zeta-potential measurement apparatus (Nihon Rufuto Co. Ltd., Japan). During the sample measurement (assuming contaminant was consisted of diluted iron oxide in aqueous), the refractive index was set at 3.22 with an absorbance value of 1.0.

2.8. Particle size measurement

The particle size of as-received and the permeated samples were measured using a Malvern ZetaSizer Nano-ZS (Malvern Instruments, UK). Each sample was measured three times before the average particle size for each sample could be determined. Owing to the soft aggregation between solid particles, NOM accumulation and fouling of the particles on the wall container, the samples were ultra-sonicated at 53 kHz for 2 min to enhance particle dispersion.

3. Results and discussion

3.1. Water characteristics and collected solid content

The characteristics of the as-received samples are shown in Table 1. The results show that all detected compounds inside the bulk follow the standard, except for the iron (elemental) material. It was noticed that the amount of iron slightly exceeded the standard limit when the treated water samples were collected from a rusted distribution system.

From the XRD analysis, the filtered solid particles or retentate (collected from as-received samples) consist of several iron-oxide polymorphs, as detailed in Fig. 2. Five different peaks of iron-oxide polymorphs were identified after calcining the retentate at 600 °C for 5 h. The retentate must be heated in order to remove the NOM that screen the solid content. The iron-oxide polymorphs were detected using XRD, whereby the major species identified were α-FeOOH at 26.4°, Fe_3O_4 at 35.5°, maghemite at 42° as well as Fe_2O_3 at 32.9° and 48.9° [15,16]. Fe_2O_3 and maghemite were detected because of the transformation of α-FeOOH and Fe_3O_4 when the susbtances were heated above 600 °C. Therefore, it was confirmed that α-FeOOH and Fe_3O_4 were the initial forms of iron oxide suspended in the water sample, which was in good agreement with previous works reported by Baek et al [17]. Legodi and De Waal [15]. Lin et al. [14] and Sarin et al. [4]. Table 2 shows the comparisons between the iron-oxide polymorphs found in the samples and the corroded iron-based pipe surfaces [17].

Table 2
Comparisons of the iron-oxide polymorphs in the collected water samples and the analysed galvanised metal pipelines from Baek et al. [17].

Corroded substance	In water samples	In pipe wall surface [17]
Hematite, α-Fe_2O_3	Available	Not available
Goethite,α-FeOOH	Available	Available
Magnetite, Fe_3O_4	Available	Available
Maghemite, γ-Fe_2O_3	Available	Available
Siderite, $FeCO_3$	Not available	Available

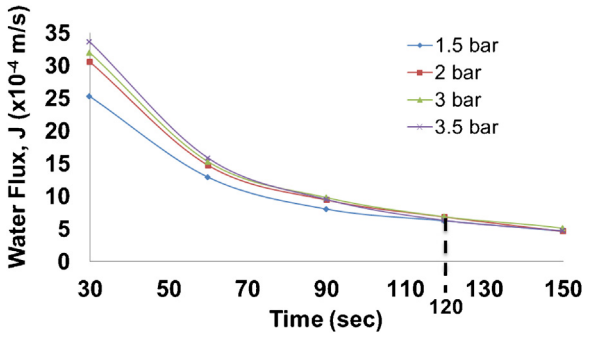

Fig. 3. Permeate flux pattern of the collected water samples with various applied pressures using a PES membrane (all samples were sonicated at 53 kHz, 2 min before the filtration process). Internal fouling occurs after 120 s.

3.2. Filtration of iron-oxide particles

The filtration process was performed using a PES membrane with a MWCO of 100 kDa. As the iron particles in the water range from 88.85 g/mol (α-FeOOH) to 231.55 g/mol (Fe_3O_4), penetration of fine particles through the PES membrane is possible. The existence of fine iron-oxide particles inside the permeate was concentrated if most of the trapped particles within the membrane matrix were released. Fig. 3 shows the effect of PES membrane filtration at various applied pressures, ranging from 1.5 to 3.5 bar. The permeate flux decreased with time, owing to the retention of solutes or particulates on the outer layer of the membrane surface during the prefilter stage. Initially, a high flux rate, 30×10^{-4} m/s, was observed when the applied pressure was higher than 1.5 bar. After 120 s, internal fouling was already dominant in the process, owing to the increase in the number of deposited particles on the membrane surface. As the applied pressure increased between 2 and 3.5 bars, the fouling was more apparent, whereby the flux exceeded the membrane limiting value, which promotes the concentration polarisation and forms a gel layer [18]. Under these conditions, the accumulated iron particles formed complex aggregates and were unable to pass through the membrane. When the critical conditions were exceeded, the excess applied pressure forced the clogged solutes to penetrate through the membrane. Fig. 4 shows the conditions under which fouling occured and the flux reached the membrane limiting flux, J_{limit}. After reaching this limiting flux, a significant increase in particle size could be clearly observed in the permeate solution (see Fig. 5). The permeate flux comparison was performed for pure water and the collected water sample to observe the fouling effect. The pure water sample did not produce any fouling or reach the membrane limiting flux, which indicates that pure water is free from fine particulates.

Here, we assumed that the transport of iron-oxide particles through the membrane pores is governed by particle motion on the membrane system, which includes a combined effect of electrostatic repulsion, Brownian forces and particle hydrodynamic drag. In normal flow filtration, the large particles are transported away from the membrane surface through lift forces, allowing one to operate filtration devices at high filtration velocities without sig-

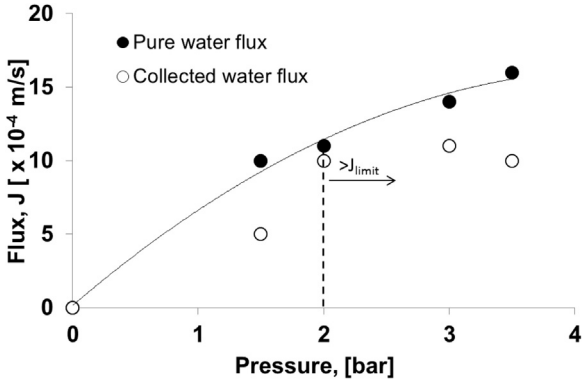

Fig. 4. Permeate flux comparison between pure water and the collected water samples under various applied pressures from 0 to 3.5 bar. Zero pressure represents the unfiltered, collected water.

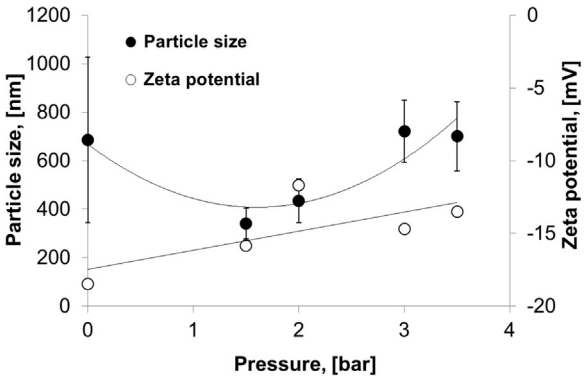

Fig. 5. Particle size and zeta potential values of the solid content in the collected water samples and the permeate. Zero pressure represents the unfiltered, collected water.

nificant fouling or polarisation. However, Kim and Zydney claimed that small particles tend to deposit on the membrane surface, as the drag force from filtration is greater than the inertial lift [19]. Brownian forces have a large effect on the particle trajectories, allowing particles to enter the pore even under conditions at which the electrostatic repulsion is greater than the hydrodynamic drag force. Below the critical filtration velocity or membrane limiting flux, the particles attain an equilibrium position above the membrane at the point whereby the hydrodynamic drag forces are exactly balanced by electrostatic repulsion. At small values of the electrostatic forces, corresponding to very high filtration velocities, the particles simply follow the fluid streamlines through the membrane. Thus, when the membrane limiting flux is exceeded, the fraction of particles entering the pores increases with increasing filtration velocity [19]. The theories were also supported by Richard et al., whereby they defined the "critical filtration velocity" or membrane limiting flux as the fluid velocity within the membrane pore at which the net force acting on a particle, located at fixed position above the pore, vanishes [20].

Fig. 5 shows the characterisation of particulates, that is, the. particle size and zeta potential values of the iron oxide in the permeate. The particle size and zeta potential of the iron-oxide particles in the water before filtering were 450 nm and −18.5 mV, respectively. After passing the water sample through a 100 kDa PES membrane at 1.5 bar, nanometer-order iron-oxide particles appeared in the water. The particle size in the permeate was 340 nm, with a zeta potential value of −13 mV. This suggested that the iron-oxide particles in the treated water were moderately stable. However, after the J_{limit} was exceeded at an applied pressure of 2 bar, the particle size in the permeate increased from 340 to 434 nm and the zeta

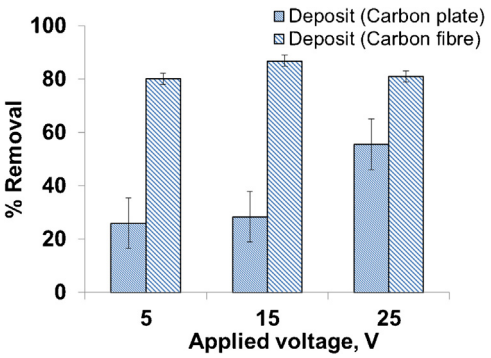

Fig. 6. Deposition of iron-oxide particles from a membrane filter on carbon-plate and carbon-fibre electrodes. A high percentage removal can be obtained using the carbon-fibre electrodes located on the cathode side.

potential values reduced from −15.14 to −11.78 mV. The aggregate size also increased from 434 to 700 nm with increasing applied pressure. Starting from 2 bar onwards, it is assumed that most of the fine particles were coming from the clogged filter matrix. In our hypothesis, aggregation of iron-oxide particle in the permeate occurred because of interparticle collisions during the concentration polarisation that promoted gel polarisation or because of the compaction of iron-oxide particles inside the membrane matrix [21]. This hypothesis is consistent with the studies reported by Harmant and Aimar and Petsev et al. [18,22].

The aggregation of iron-oxide particles could also be attributed to multi-polar surface charge interactions that contribute to partial neutralisation inside the membrane matrix. The multi-polar surface charge occurs because of the presence of adsorbed contaminants such as natural organic matter (NOM) and other adsorbed metal arsenic that shifts the zeta potential values [23,24]. In addition, free ions such as Na^+, Ca^{2+} and K^+ that were present in the water samples could also cause multi-polar surface charging. The ions were subjected to a shielding effect in the electrical double layer of the iron-oxide particles (thinner electrical double layer) in the water, thus reducing the zeta potential value [25].

3.3. Deposition and removal percentage

Fig. 6 shows the removal of iron particles in water samples using two different types of substrates, a carbon plate and activated carbon filter. The difference between these two substrates is the deposition rate, owing to the substrate morphology and surface area. The carbon plate in this study is a rigid material, whereas carbon fibre is more flexible and exists in fibrous form. The carbon filter offered a higher surface area compared to the carbon plate substrate, owing to the fibre arrangement. The FESEM images of the carbon fibre before and after EPD are shown in Fig. 7. A low applied potential is preferable in this study, because a high level of gas formation is observed at the high voltage. The amount of deposited particles increased as the applied potential increased, suggesting that the yield or deposits follow the EPD model, as predicted by Biesheuvel et al. and in from our previous work [26,29,30]. Owing to water electrolysis, particular concern should be given to the bubbles produced in the vicinity of the substrates, because it could affect the particle deposition uniformity [27,30]. Optimum removal occurs at <25 V, where 80–87% removal was obtained using the carbon fibre, whereas 26–56% removal was achieved using the carbon plates. The obtained particles with moderate zeta potential values were stable in the suspension and could deposit during the EPD process.

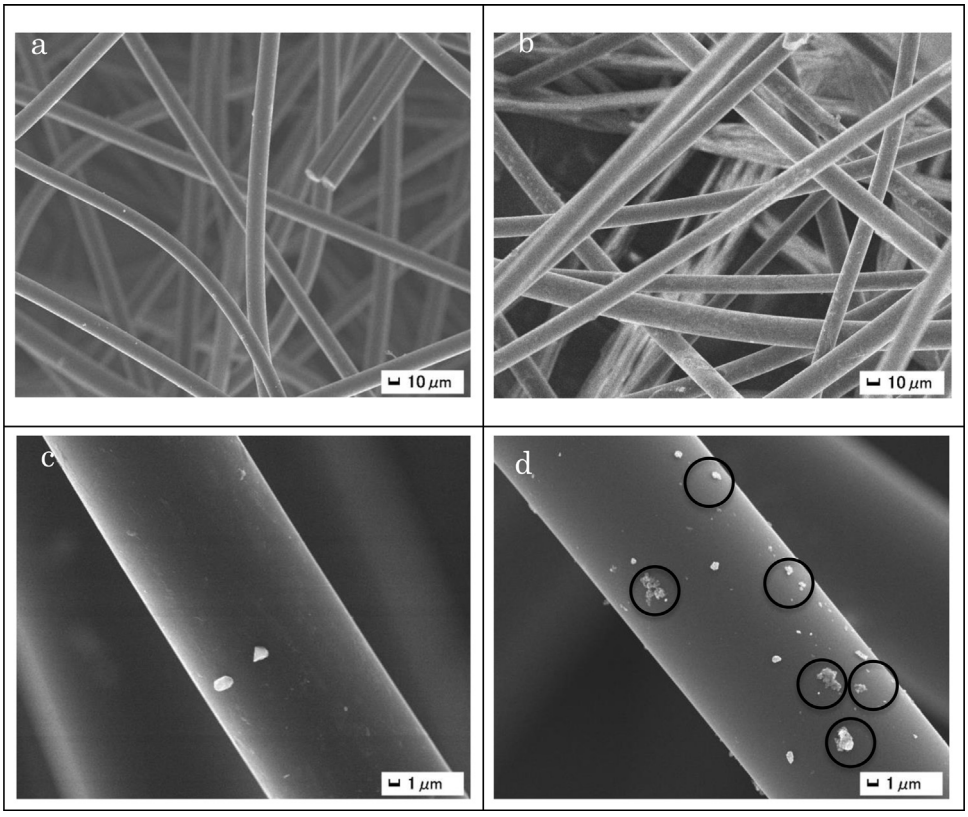

Fig. 7. FESEM images of the carbon-fibre electrodes a before and b after deposition. Magnification of the fibre strands c before and d after the deposition (deposit particles is indicated with round circles).

4. Conclusion

Throughout this study, it is proven that drinking water from the specific distribution system:

1. Consists of the mentioned iron-oxide polymorphs hematite, magnetite and maghemite.
2. Contains particles that tend to aggregate because of compaction inside the membrane filter matrix when the iron-oxide particles pass through the filtration system with an applied pressure higher than J_{limit}.
3. Consists of penetrated iron oxide in the permeate region with moderate—low zeta potential values, which get lower as they exceed J_{limit}.
4. Has a high percentage removal of up to 87% when using a high-surface-area substrate with a 2 cm electrode distance and 5–25 V applied potential.
5. Contains iron particles with high zeta potential value that can be efficiently removed using electrophoretic deposition method; however, those with a low zeta-potential value close to zero are unable to deposit.

Acknowledgements

The authors are grateful to Dr. Rajagopalan Prabu for his technical contribution and Ms. Syahira Mohd. Sharif for the experimental setup. This study was supported by Universiti Putra Malaysia, Universiti Teknologi MARA (UiTM) and Ministry of Education Malaysia through financial support of Universiti Putra Malaysia Grant (GP-IPS/2013/9399815), UiTM Research Entity Initiative (REI) Tier5 Grant (600-RMI/DANA 5/3 REI (2/2013)) and Fundamental Research Grants Scheme (FRGS/2/2013/TK05/UPM/02/15).

References

[1] S. Dixit, J.G. Hering, Comparison of arsenic (V) and arsenic (III) sorption onto iron oxide minerals: implications for arsenic mobility, Environ. Sci. Technol. 37 (2003) 4182–4189.
[2] D.A. Lytle, V.L. Snoeyink, Effect of *ortho*-and polyphosphates on the properties of iron particles and suspensions, J.-Am. Water Works Assoc. 94 (2002) 87–99.
[3] K. Emde, D. Smith, R. Facey, Initial investigation of microbially influenced corrosion (MIC) in a low-temperature water distribution system, Water Res. 26 (1992) 169–175.
[4] P. Sarin, V. Snoeyink, J. Bebee, K. Jim, M. Beckett, W. Kriven, J. Clement, Iron release from corroded iron pipes in drinking water distribution systems: effect of dissolved oxygen, Water Res. 38 (2004) 1259–1269.
[5] T.L. Gerke, J.B. Maynard, M.R. Schock, D.L. Lytle, Physiochemical characterization of five iron tubercles from a single drinking water distribution system: possible new insights on their formation and growth, Corros. Sci. 50 (2008) 2030–2039.
[6] F.E. Senftle, A.N. Thorpe, J.R. Grant, A. Barkatt, Superparamagnetic nanoparticles in tap water, Water Res. 41 (2007) 3005–3011.
[7] N.F. Gray, Problem arising from water treatment Drinking Water Quality: Problems and Solutions, vol. 1, John Wiley and Sons, Ltd., United States of America, 1994, pp. 315.
[8] A. Seth, R. Edyvean, The function of sulfate-reducing bacteria in corrosion of potable water mains, Int. Biodeterior. Biodegr. 58 (2006) 108–111.
[9] J. Świetlik, U. Raczyk-Stanisławiak, P. Piszora, J. Nawrocki, Corrosion in drinking water pipes: the importance of green rusts, Water Res. 46 (2012) 1–10.
[10] K.P. Raven, A. Jain, R.H. Loeppert, Arsenite and arsenate adsorption on ferrihydrite: kinetics, equilibrium, and adsorption envelopes, Environ. Sci. Technol. 32 (1998) 344–349.
[11] R.W. Field, E.L. Fisher, R.L. Valentine, B.C. Kross, Radium-bearing pipe scale deposits: implications for national waterborne radon sampling methods, Am. J. Public Health 85 (1995) 567–570.
[12] M.N. Naim, M. Iijima, K. Sasaki, M. Kuwata, H. Kamiya, I.W. Lenggoro, Electrical-driven disaggregation of the two-dimensional assembly of colloidal polymer particles under pulse DC charging, Adv. Powder Technol. 21 (2010) 534–541.
[13] A. Schäfer, U. Schwicker, M. Fischer, A.G. Fane, T. Waite, Microfiltration of colloids and natural organic matter, J. Membr. Sci. 171 (2000) 151–172.
[14] H.Y. Lin, Y.-W. Chen, W.-J. Wang, Preparation of nanosized iron oxide and its application in low temperature CO oxidation, J. Nanopart. Res. 7 (2005) 249–263.

[15] D. Legodi, M. De Waal, Raman spectroscopic study of ancient South African domestic clay pottery, Spectrochim. Acta Part A: Mol. Biomol. Spectrosc. 66 (2007) 135–142.
[16] Z. Zhang, J.E. Stout, V.L. Yu, R. Vidic, Effect of pipe corrosion scales on chlorine dioxide consumption in drinking water distribution systems, Water Res. 42 (2008) 129–136.
[17] Y. Baek, J. Kang, P. Theato, J. Yoon, Measuring hydrophilicity of RO membranes by contact angles via sessile drop and captive bubble method: a comparative study, Desalination 303 (2012) 23–28.
[18] P. Harmant, P. Aimar, Coagulation of colloids in a boundary layer during cross-flow filtration, Colloids Surf. A: Physicochem. Eng. Aspects 138 (1998) 217–230.
[19] M. Kim, A.L. Zydney, Effect of electrostatic, hydrodynamic, and Brownian forces on particle trajectories and sieving in normal flow filtration, J. Colloid Interface Sci. 269 (2004) 425–431.
[20] W. Richard Bowen, A.N. Filippov, A.O. Sharif, V.M. Starov, A model of the interaction between a charged particle and a pore in a charged membrane surface, Adv. Colloid Interface Sci. 81 (1999) 35–72.
[21] C.Y. Tang, T. Chong, A.G. Fane, Colloidal interactions and fouling of NF and RO membranes: a review, Adv. Colloid Interface Sci. 164 (2011) 126–143.
[22] D. Petsev, V. Starov, I. Ivanov, Concentrated dispersions of charged colloidal particles: sedimentation, ultrafiltration and diffusion, Colloids Surf. A: Physicochem. Eng. Aspects 81 (1993) 65–81.
[23] M. Erdemoğlu, M. Sarıkaya, M. Canbazoğlu, Leaching of celestite with sodium sulfide, J. Dispers. Sci. Technol. 27 (2006) 439–442.
[24] A.S. Jönsson, B. Jönsson, Ultrafiltration of colloidal dispersions—a theoretical model of the concentration polarization phenomena, J. Colloid Interface Sci. 180 (1996) 504–518.
[25] P. Lakshmipathiraj, B. Narasimhan, S. Prabhakar, G. Bhaskar Raju, Adsorption of arsenate on synthetic goethite from aqueous solutions, J. Hazard. Mater. 136 (2006) 281–287.
[26] P.M. Biesheuvel, H. Verweij, Theory of cast formation in electrophoretic deposition, J. Am. Ceram. Soc. 82 (6) (1999) 1451–1455.
[27] I.A. Alam, M. Sadiq, Metal contamination of drinking water from corrosion of distribution pipes, Environ. Pollut. 57 (1989) 167–178.
[28] Ministry of Health, Malaysia, National Guideline for Drinking Water Quality (W. H. Organization, ed.), Vol. Twenty-Fifth Schedule (Regulation 394 (1) and 360 B(3), Standard for Water and packaged drinking water, Food Act 1983 (Act 281), Food Regulation, 1985. Drinking Water Quality Surveillance Unit, Division of Engineering Services, Kuala Lumpur.
[29] K. Kusdianto, M. Nazli Naim, Keitaro Sasaki, I. Wuled Lenggoro, Immobilization of colloidal particles into sub-100 nm porousstructures by electrophoretic methods in aqueous media, Colloids Surf. A: Physicochem. Eng. Aspects 459 (2014) 142–150.
[30] S. Mohd Sharif, N.M. Abu Bakar, M. Nazli Naim, Deposition of fine iron oxide particles in tap water using electrophoretic deposition technique (EPD), J. Water Process Eng. 7 (2015) 123–130.